Magnetization Process and Collective Excitations in the $S = 1/2$ Triangular-Lattice Heisenberg Antiferromagnet $Ba_3CoSb_2O_9$

Takuya Susuki,[1] Nobuyuki Kurita,[1] Takuya Tanaka,[2] Hiroyuki Nojiri,[2] Akira Matsuo,[3] Koichi Kindo,[3] and Hidekazu Tanaka[1]

[1]*Department of Physics, Tokyo Institute of Technology, Meguro-ku, Tokyo 152-8551, Japan*
[2]*Institute for Material Research, Tohoku University, Aoba-ku, Sendai 980-8577, Japan*
[3]*Institute for Solid State Physics, University of Tokyo, Kashiwa, Chiba 277-8581, Japan*

(Received 17 March 2013; published 24 June 2013)

We have performed high-field magnetization and electronic spin resonance (ESR) measurements on $Ba_3CoSb_2O_9$ single crystals, which approximates the two-dimensional (2D) $S = 1/2$ triangular-lattice Heisenberg antiferromagnet. For an applied magnetic field H parallel to the ab plane, the entire magnetization curve including the plateau at one-third of the saturation magnetization (M_s) is in excellent agreement with the results of theoretical calculations except a small step anomaly near $(3/5)M_s$, indicative of a theoretically undiscovered quantum phase transition. However, for $H \parallel c$, the magnetization curve exhibits a cusp near $M_s/3$ owing to the weak easy-plane anisotropy and the 2D quantum fluctuation. From a detailed analysis of the collective ESR modes observed in the ordered state, combined with the magnetization process, we have determined all the magnetic parameters including the interlayer and anisotropic exchange interactions.

DOI: 10.1103/PhysRevLett.110.267201 PACS numbers: 75.10.Jm, 75.45.+j, 75.60.Ej, 76.30.−v

Over the past decades, there has been considerable interest in frustrated quantum magnets, owing to a rich variety of exotic quantum phenomena [1–3]. For classical spins with an antiferromagnetic coupling, a geometric frustration suppresses the long-range ordering, leading to a degenerate ground state. The degeneracy can be destroyed by quantum fluctuations, which emerge not only through an interplay of strong geometric frustration, low dimensionality, and small spin but also through the application of a magnetic field. Despite intensive research efforts, the detailed mechanism of the quantum effects, e.g., the ground state property [4,5], has still been highly controversial.

One macroscopic manifestation of the quantum phenomena is the stabilization of the ''up-up-down'' spin structure under a magnetic field, predicted for a two-dimensional (2D) triangular-lattice Heisenberg antiferromagnet (TLHAF) with a small spin [6,7]. In a magnetization process, the nonclassical anomaly appears as a plateau in a finite field range at one-third of the saturation magnetization M_s, hereafter referred to as the $M_s/3$ plateau. In a classical picture, a monotonic increase in the magnetization is expected up to M_s. A number of theoretical approaches for explaining the quantum mechanism of the $M_s/3$ plateau have been proposed [8–14]. Thus far, however, few numbers of definite experimental results reserved judgment on the issue. This is mainly due to the experimental difficulty in growing the model material, let alone in observing the $M_s/3$ plateau purely driven by quantum fluctuations. In fact, most of the TLHAFs ever studied, such as Cs_2CuBr_4 [15,16], have a distorted triangular lattice, which induces an antisymmetric Dzyaloshinsky-Moriya interaction.

It is believed that the spin state in the lower-field range above the higher edge field of the $M_s/3$ plateau is the 2:1 canted coplanar state that is a continuous variant of the up-up-down state [7–11]. However, whether the 2:1 canted coplanar state is stable up to the saturation or a new quantum spin state emerges in higher-field range is still unclear [17]. To conduct the quantitatively verification of the theory and the elucidation of the high-field spin state, the experimental realization of a 2D $S = 1/2$ Heisenberg antiferromagnet on a uniform triangular lattice is necessary.

Recently, we have demonstrated that $Ba_3CoSb_2O_9$ enables us to experimentally investigate a 2D $S = 1/2$ TLHAF system [18]. Magnetic Co^{2+} ions form uniform triangular-lattice layers parallel to the ab plane [19,20]. Since the magnetic layers are separated by nonmagnetic layers consisting of the Sb_2O_9 double octahedron and Ba^{2+} ions, the intralayer exchange interaction is expected to be dominant. On the other hand, the antiferromagnetic ordering at the Néel temperature $T_N \approx 3.8$ K [18,20] is due to the weak interlayer exchange interaction. The Dzyaloshinsky-Moriya interaction is absent in $Ba_3CoSb_2O_9$ because of the highly symmetric crystal structure with the space group $P6_3/mmc$. The effective magnetic moment of Co^{2+} ions, which possess the true spin $S = 3/2$, can be described by the pseudospin-1/2 at low temperatures well below $|\lambda|/k_B \approx 250$ K (λ: spin orbit coupling constant) [21,22]. Thus, the $M_s/3$ plateau observed using $Ba_3CoSb_2O_9$ powder samples in Ref. [18] could be attributed only to the quantum fluctuations.

Many experimental spin-1/2 systems are composed of a Cu^{2+} ion that has true spin $S = 1/2$. However, it is

impossible to realize a regular triangular lattice composed of Cu^{2+} ions, because the orbital degeneracy cannot be lifted in trigonal crystal field, and thus, the trigonal (or hexagonal) crystal lattice is unstable at low temperatures. Therefore, $Ba_3CoSb_2O_9$ is a rare experimental system of $S = 1/2$ antiferromagnet on a uniform triangular lattice, and thus, it is important to perform more precise experiments on $Ba_3CoSb_2O_9$.

In this Letter, we present single-crystal studies of $Ba_3CoSb_2O_9$, performed by the high-field magnetization and electron spin resonance (ESR) measurements. For magnetization processes, a quantum $M_s/3$ plateau is clearly observed for $H \parallel ab$, whereas for $H \parallel c$, the magnetization curve exhibits a cusp near $M_s/3$. We have found a small magnetization anomaly near $(3/5)M_s$ for $H \parallel ab$, which indicates the emergence of a new high-field phase stabilized by the quantum fluctuation. ESR has proven to be an excellent probe of collective excitation modes with a high sensitivity, which could provide a significant clue to the configuration of spin triangles. As shown below, the ESR modes observed for $H \parallel c$, together with the magnetization process depending on the field direction, indicate that $Ba_3CoSb_2O_9$ is close to the ideal 2D $S = 1/2$ TLHAF with a weak easy-plane anisotropy.

Single crystals of $Ba_3CoSb_2O_9$ were grown from the melt using a Pt tube as a crucible. $Ba_3CoSb_2O_9$ powder, which was prepared by the same procedure described in the previous Letter [18], was packed into the Pt tube. The temperature of the furnace was reduced from 1700 to 1600 °C for 3 days. High-field magnetization processes at pulsed magnetic fields up to 47 T were measured at $T = 1.3$ K($< T_N \approx 3.8$ K) at the Institute for Solid State Physics, University of Tokyo. High-frequency ESR measurements at pulsed magnetic fields up to 13 T with fixed frequencies ranging from 55 to 405 GHz were performed in the temperature range of 1.6–20 K at the Institute for Materials Research, Tohoku University. Usually, the ESR signal of Co^{2+} in the octahedral environment is hard to observe at high temperatures because of the short spin-lattice relaxation time. Therefore, we performed the ESR measurements at helium temperatures, where the spin-lattice relaxation time becomes long enough to observe well-defined ESR signals, as shown below. For both measurements, we stacked several pieces of plate-shaped samples with typical dimensions of $\sim 2 \times 2 \times 0.5$ mm^3. The wide faces were found to be the ab plane by x-ray single-crystal diffraction. Magnetic fields were applied parallel to the ab plane and c axis.

Figure 1 shows the raw magnetization M_{raw} (left) and its field derivative dM_{raw}/dH (right) as a function of H in $Ba_3CoSb_2O_9$ single crystals. The anomaly observed at around 4 T in dM_{raw}/dH is due to an instrumental problem. The saturation field H_s is obtained to be 31.9 and 32.8 T for $H \parallel ab$ and $H \parallel c$, respectively. The absolute values of the magnetization were calibrated with g factors determined as $g = 3.84$ and 3.87 for $H \parallel ab$ and $H \parallel c$, respectively, by the present electron paramagnetic resonance (EPR) measurements performed at 20 K (see the inset in Fig. 3). The magnetic moment of Co^{2+} in $Ba_3CoSb_2O_9$ is almost isotropic, unlike that in typical Co compounds [21]. The saturation magnetization M_s is determined as 1.93 and $1.94\mu_B/Co^{2+}$ for $H \parallel ab$ and $H \parallel c$, respectively. The H_s and M_s values are both consistent with those obtained from our previous results of powder samples [18]. The continuous increase in M_{raw} above H_s is attributed to the large Van Vleck paramagnetism characteristic of Co^{2+} in the octahedral environment [21,22]. From the magnetization slopes above H_s, the Van Vleck paramagnetic susceptibility is determined as $\chi_{\mathrm{VV}} = 1.59 \times 10^{-2}$ and $1.90 \times 10^{-2}(\mu_B/T)/Co^{2+}$ for $H \parallel ab$ and $H \parallel c$, respectively. It is noted that the magnetization anomalies around H_s and the $M_s/3$ plateau for $H \parallel ab$ are more distinctly observed as compared with the previous results obtained for powder samples [18], as can also be observed from the sharp anomalies in dM_{raw}/dH data.

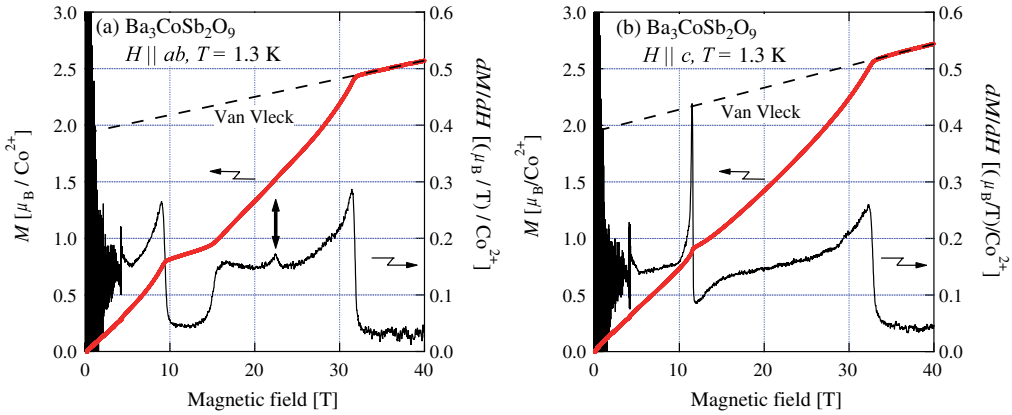

FIG. 1 (color online). Field dependence of the raw magnetization M_{raw} (left) and its field derivative dM_{raw}/dH (right) in $Ba_3CoSb_2O_9$ single crystals, measured at 1.3 K for (a) $H \parallel ab$ and (b) $H \parallel c$. Dashed lines denote the Van Vleck paramagnetism. A double-headed arrow in (a) indicates an anomaly near $3/5M_s$, possibly related to the spin rearrangement.

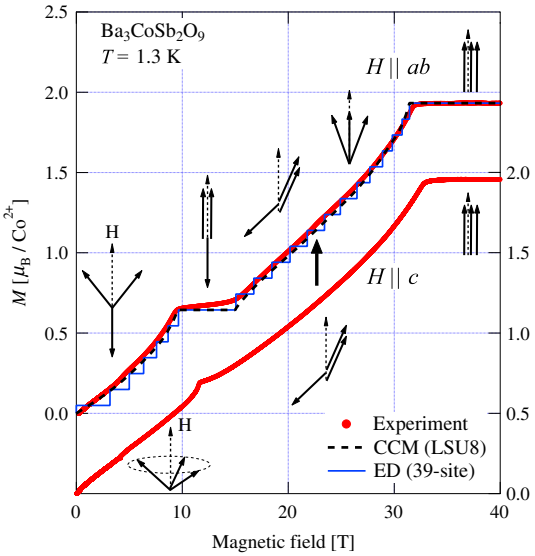

FIG. 2 (color online). Magnetization curves in $Ba_3CoSb_2O_9$ at 1.3 K for $H \parallel ab$ (left) and $H \parallel c$ (right), corrected for the Van Vleck paramagnetism. The dashed curve and steplike line denote the results calculated by a higher-order coupled cluster method (CCM) [11] and exact diagonalization (ED) for a 39-site rhombic cluster [14], respectively. Spin structures at various magnetic fields are illustrated.

Figure 2 shows the magnetization curves corrected for the Van Vleck terms. For $H \parallel ab$, a quantum magnetization plateau is clearly observed at $M \simeq M_s/3$. For comparison, theoretical magnetization curves are also displayed. Thick dashed and solid lines are the magnetization curves calculated by a higher-order CCM [11] and ED for a 39-site rhombic cluster [14], respectively. Both calculations excellently reproduce the experimental magnetization processes for $H \parallel ab$ despite the fact that the adjustable parameters are only H_s and M_s. The field range of the experimental $M_s/3$ plateau is evaluated to be $0.30 \leq H/H_s \leq 0.47$, which is almost identical to $0.306 \leq H/H_s \leq 0.479$ obtained by CCM [11] and ED [14].

For a 2D $S = 1/2$ TLHAF, the quantum up-up-down spin state is predicted to emerge, irrespective of the applied field direction. In $Ba_3CoSb_2O_9$, however, the magnetization curve for $H \parallel c$ exhibits a cusp at $(H, M) = (11.6[T], 0.66[\mu_B/Co^{2+}]) \approx (H_s/3, M_s/3)$. The absence of the $M_s/3$ plateau phase for $H \parallel c$ should be ascribed to the weak planar anisotropy in $Ba_3CoSb_2O_9$. It has been reported that hexagonal $CsCuCl_3$, which is described as a ferromagnetically stacked triangular-lattice antiferromagnet with a small planar anisotropy due to the Dzyaloshinsky-Moriya interaction and the anisotropic exchange interaction [23], shows similar magnetization behaviors, namely, an ill-defined $M_s/3$ plateaulike anomaly for $H \parallel ab$ and a small jump for $H \parallel c$ at around $H_s/3$ [24]. By analogy with $CsCuCl_3$, the magnetic anisotropy in $Ba_3CoSb_2O_9$ should be of the easy-plane type, which will also be confirmed by the analysis of the collective ESR modes, as shown below.

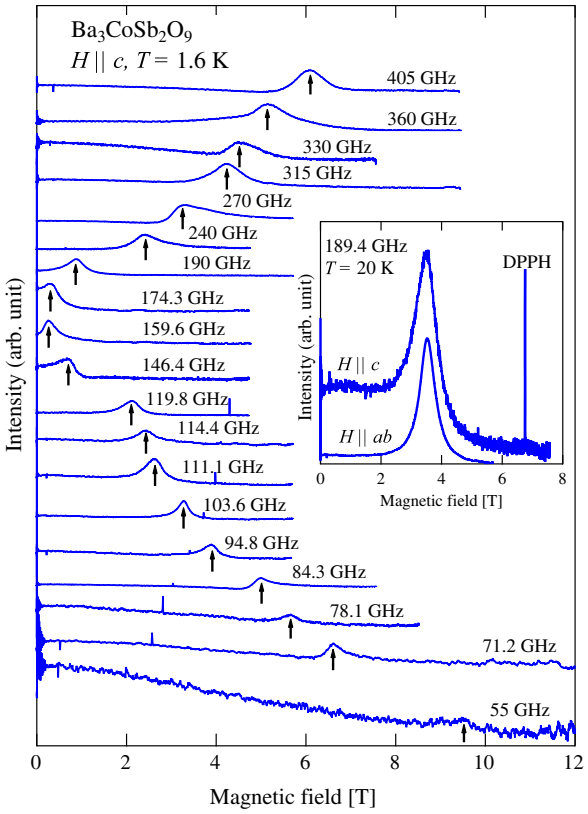

FIG. 3 (color online). ESR spectra of $Ba_3CoSb_2O_9$ measured at 1.6 K ($< T_N$) for $H \parallel c$. Arrows indicate resonance fields. The inset shows an expanded view of the paramagnetic resonance (EPR) spectra measured for $H \parallel ab$ and $H \parallel c$ at 20 K ($> T_N$) and 189.4 GHz, where a sharp line labeled DPPH indicates $g = 2$.

The spin structure expected in each magnetic phase in $Ba_3CoSb_2O_9$ is illustrated in Fig. 2. At zero magnetic field, the spins induce the 120° coplanar ordering in the ab plane. As a magnetic field is applied for $H \parallel ab$, the quantum up-up-down state with $M = M_s/3$ is stabilized for $0.297 \leq H/H_s \leq 0.472$, followed by the 2:1 canted coplanar phase at higher magnetic fields, skipping the up-up-down state. For $H \parallel c$, on the other hand, a phase transition occurs at $H \simeq H_s/3$ from the low-field umbrella structure, which gains the anisotropy energy of the easy-plane type, to the high field 2:1 canted coplanar one. In the 3D case, this transition accompanies a small magnetization jump [8,24]. However, in $Ba_3CoSb_2O_9$, the magnetization exhibits a cusp anomaly. We infer that the 2D quantum fluctuation changes the magnetization jump into the cusp.

As indicated by a double-headed arrow in Fig. 1(a), one can see a small magnetization anomaly at around $1.5[\mu_B/Co^{2+}] \approx (3/5)M_s$ for $H \parallel ab$, which appears as a clear peak in the dM/dH curve. Such a magnetization anomaly was not detected for $H \parallel c$ [25]. The magnetization anomaly near $(3/5)M_s$ is indicative of the emergence of a new high-field quantum phase. This means that different from the theoretical expectation, the 2:1 canted

coplanar state is not stable up to the saturation. One possibility of the high-field phase is a high-symmetric coplanar phase as shown in Fig. 2, in which one of the three sublattice spins is aligned along the applied field [17]. To determine the high-field spin structure, additional measurements, such as a nuclear magnetic resonance measurement, are required.

Next, we present the results of multifrequency high-field ESR measurements on $Ba_3CoSb_2O_9$ to provide more clues to the spin configurations and magnetic parameters through the collective magnetic excitations in the ordered state. The main panel of Fig. 3 shows the field dependence of ESR spectra at 1.6 K measured for $H \parallel c$ at various fixed frequencies up to 405 GHz. As indicated by arrows, each ESR spectrum in the investigated frequency range has one clear absorption signal, although the spectrum at 55 GHz is noisy. The inset in Fig. 3 shows the paramagnetic resonance (EPR) spectra measured for $H \parallel ab$ and $H \parallel c$ at 20 K ($> T_N$) and 189.4 GHz. From the resonance fields of the EPR, the g factors were determined as $g = 3.84$ and 3.87 for $H \parallel ab$ and $H \parallel c$, respectively. Such an almost isotropic g factor is rare for Co^{2+} in the octahedral environment.

The resonance data obtained are summarized in the frequency-field diagram shown in Fig. 4. Open and solid symbols represent the collective ESR modes (1.6 K) and EPR (20 K) data, respectively. The collective ESR modes consist of two distinct branches labeled as ω_+ and ω_-. At zero magnetic field, the two modes appear to be degenerate with an energy gap of approximately 170 GHz. As the magnetic field increases, the energy of the ω_+ mode increases and tends to approach the EPR line with $g = 3.87$, whereas the energy of the ω_- mode decreases monotonically toward zero. The field evolutions of the ω_+ and ω_- modes for $H \parallel c$ are characteristic of the triangular-lattice antiferromagnet with the easy-plane anisotropy rather than the easy-axis one [26–28]. If the anisotropy is of the easy-axis type, no degeneracy of the ω_+ and ω_- modes occurs at zero magnetic field.

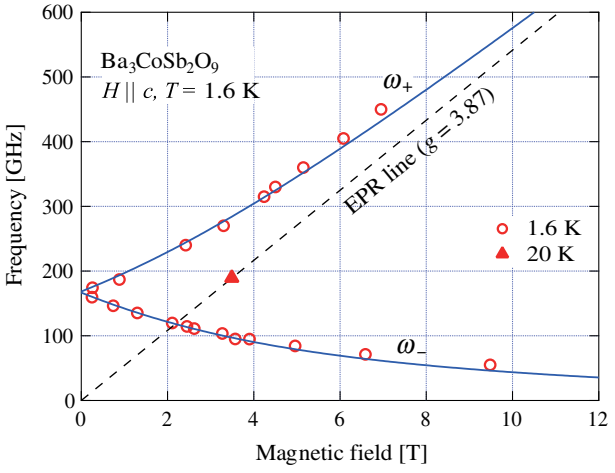

FIG. 4 (color online). Frequency-field diagram of the collective ESR modes in $Ba_3CoSb_2O_9$ for $H \parallel c$. Open symbols denote the resonance points obtained at 1.6 K, where the upper and lower frequency modes are labeled as ω_+ and ω_-, respectively. Solid curves are fits with Eq. (1) based on a six-sublattice model (see text). Solid symbols indicate the EPR data measured for $H \parallel c$ at 20 K. The dashed line is the EPR line described with $g = 3.87$.

Here, we analyze the collective ESR modes for $H \parallel c$ in $Ba_3CoSb_2O_9$. We consider six sublattices, because the neighboring triangular layers are antiferromagnetically coupled [20]. The resonance conditions can be derived analytically by solving the torque equations for the six-sublattice model as

$$\hbar\omega_{\pm} = \sqrt{\left(4J' + \frac{9}{2}J\right)\left\{\frac{3\Delta J}{4} + \frac{(8J' + 9J - 6\Delta J)}{2(4J' + 9J + 3\Delta J)^2}(g\mu_B H)^2\right\}} \pm \frac{9J}{8J' + 18J + 6\Delta J} g\mu_B H, \quad (1)$$

where J and J' are the intralayer and interlayer exchange constants, respectively, and ΔJ is the coefficient of anisotropic exchange interaction in the layer defined as $\Delta J(S_i^x S_j^x + S_i^y S_j^y)$. The resonance conditions of Eq. (1) are the same as those obtained from the linear spin wave theory. Because the intralayer exchange interaction is dominant, the condition $J \gg \Delta J,\ J'$ is satisfied in $Ba_3CoSb_2O_9$.

The intralayer exchange constant J was evaluated to be $J/k_B = 18.5$ K from the saturation fields H_s for $H \parallel ab$ and $H \parallel c$ using the relation $g\mu_B H_s = 9J/2$. In the analysis, we fixed the value of J and the g factor of 3.87 obtained via the EPR measurement for $H \parallel c$. Solid curves in Fig. 4 are fits obtained using Eq. (1) with $J'/k_B = 0.48$ K and $\Delta J/k_B = 1.02$ K, which are sufficiently smaller than J. The agreement between the experimental and theoretical results is excellent. The ESR results indicate that, in $Ba_3CoSb_2O_9$, the intralayer exchange interaction is dominant over the interlayer one and that the magnetic anisotropy is small and is of the easy-plane type, which is in disagreement with the recent report by Zhou *et al.* [29].

In Ref. [18], we proposed that $Ba_3CoSb_2O_9$ has the easy-axis anisotropy, deduced from the three-step specific heat anomaly around $T_N \approx 3.8$ K at zero magnetic field. However, three specific heat peaks measured by the relaxation method around T_N were extremely high, considering that the phase transition is of the second order. We infer that the specific heat anomaly arises from a weak first-order phase transition accompanied by the latent heat, as predicted for the XY and Heisenberg triangular-lattice antiferromagnets [30,31].

To conclude, the high-field magnetization and ESR of $Ba_3CoSb_2O_9$ single crystals have been investigated. A quantum $M_s/3$ plateau is clearly observed for $H \parallel ab$, whereas for $H \parallel c$ the magnetization curve exhibits a cusp near $H_s/3$. The suppression of the $M_s/3$ plateau for

$H \parallel c$ is ascribed to the easy-plane anisotropy. We have found a small magnetization step at nearly $(3/5)M_s$ for $H \parallel ab$, indicative of a new high-field quantum phase, which has not been predicted so far. The expected spin configurations are proposed as shown in Fig. 2. Nearly isotropic g factors of 3.84 and 3.87 are obtained for $H \parallel ab$ and $H \parallel c$, respectively, from the EPR spectrum at 20 K. From the detailed analysis of two distinct ESR modes observed for $H \parallel c$ ($T < T_N$), combined with the obtained magnetization processes, we determined interaction parameters in $Ba_3CoSb_2O_9$ with accuracy as $J/k_B = 18.5$ K, $J'/k_B = 0.48$ K, and $\Delta J/k_B = 1.02$ K. This result indicates that $Ba_3CoSb_2O_9$ closely approximates the ideal two-dimensional $S = 1/2$ TLHAF. These interaction parameters are necessary for the quantitative discussion of the quantum aspects of magnetic excitations such as negative quantum renormalization of excitation energies and the unusual singularity of dispersion relation predicted for the $S = 1/2$ TLHAF [32–34].

We would like to thank D. J. J. Farnell, R. Zinke, J. Schulenburg, J. Richter, H. Nakano, T. Sakai, and D. Yamamoto for showing us their theoretical calculations of the magnetization processes and for fruitful discussion. This work was supported by a Grant-in-Aid for Scientific Research (A) from the Japan Society for the Promotion of Science and the Global COE Program "Nanoscience and Quantum Physics" at Tokyo Tech. funded by the Ministry of Education, Culture, Sports, Science and Technology of Japan. H. T. was supported by a grant from the Mitsubishi Foundation.

[1] P. W. Anderson, Mater. Res. Bull. **8**, 153 (1973).
[2] V. Kalmeyer and R. B. Laughlin, Phys. Rev. Lett. **59**, 2095 (1987).
[3] L. Balents, Nature (London) **464**, 199 (2010).
[4] S. Yamashita, Y. Nakazawa, M. Oguni, Y. Oshima, H. Nojiri, Y. Shimizu, K. Miyagawa, and K. Kanoda, Nat. Phys. **4**, 459 (2008).
[5] M. Yamashita, N. Nakata, Y. Kasahara, T. Sasaki, N. Yoneyama, N. Kobayashi, S. Fujimoto, T. Shibauchi, and Y. Matsuda, Nat. Phys. **5**, 44 (2009).
[6] H. Nishimori and S. Miyashita, J. Phys. Soc. Jpn. **55**, 4448 (1986).
[7] A. V. Chubukov and D. I. Golosov, J. Phys. Condens. Matter **3**, 69 (1991).
[8] T. Nikuni and H. Shiba, J. Phys. Soc. Jpn. **62**, 3268 (1993).
[9] J. Alicea, A. V. Chubukov, and O. A. Starykh, Phys. Rev. Lett. **102**, 137201 (2009).
[10] J. Takano, H. Tsunetsugu, and M. E. Zhitomirsky, J. Phys. Conf. Ser. **320**, 012011 (2011).
[11] D. J. J. Farnell, R. Zinke, J. Schulenburg, and J. Richter, J. Phys. Condens. Matter **21**, 406002 (2009).
[12] A. Honecker, J. Phys. Condens. Matter **11**, 4697 (1999).
[13] A. Honecker, J. Schulenburg, and J. Richter, J. Phys. Condens. Matter **16**, S749 (2004).
[14] T. Sakai and H. Nakano, Phys. Rev. B **83**, 100405(R) (2011).
[15] T. Ono, H. Tanaka, H. A. Katori, F. Ishikawa, H. Mitamura, and T. Goto, Phys. Rev. B **67**, 104431 (2003).
[16] N. A. Fortune, S. T. Hannahs, Y. Yoshida, T. E. Sherline, T. Ono, H. Tanaka, and Y. Takano, Phys. Rev. Lett. **102**, 257201 (2009).
[17] T. Nikuni and H. Shiba, J. Phys. Soc. Jpn. **64**, 3471 (1995).
[18] Y. Shirata, H. Tanaka, A. Matsuo, and K. Kindo, Phys. Rev. Lett. **108**, 057205 (2012).
[19] U. Treiber and S. Kemmler-Sack, Z. Anorg. Allg. Chem. **487**, 161 (1982).
[20] Y. Doi, Y. Hinatsu, and K. Ohoyama, J. Phys. Condens. Matter **16**, 8923 (2004).
[21] M. E. Lines, Phys. Rev. **131**, 546 (1963).
[22] H. Shiba, Y. Ueda, K. Okunishi, S. Kimura, and K. Kindo, J. Phys. Soc. Jpn. **72**, 2326 (2003).
[23] K. Adachi, N. Achiwa, and M. Mekata, J. Phys. Soc. Jpn. **49**, 545 (1980).
[24] H. Nojiri, Y. Tokunaga, and M. Motokawa, J. Phys. (Paris) **49**, C8-1459 (1988).
[25] The dM/dH curve for the powder sample reported in Ref. [18] exhibits a tiny cusp anomaly at $H \simeq 22$ T indicative of a phase transition near $(3/5)M_s$.
[26] H. Tanaka, S. Teraoka, E. Kakehashi, K. Iio, and K. Nagata, J. Phys. Soc. Jpn. **57**, 3979 (1988); **60**, 2484 (1991).
[27] W. Palme, F. Mertens, O. Born, B. Lüthi, and U. Schotte, Solid State Commun. **76**, 873 (1990).
[28] H. Tanaka, U. Schotte, and K. D. Schotte, J. Phys. Soc. Jpn. **61**, 1344 (1992).
[29] H. D. Zhou, C. Xu, A. M. Hallas, H. J. Silverstein, C. R. Wiebe, I. Umegaki, J. Q. Yan, T. P. Murphy, J.-H. Park, Y. Qiu, J. R. D. Copley, J. S. Gardner, and Y. Takano, Phys. Rev. Lett. **109**, 267206 (2012).
[30] G. Zumbach, Phys. Rev. Lett. **71**, 2421 (1993).
[31] D. Loison and K. D. Schotte, Eur. Phys. J. B **5**, 735 (1998).
[32] O. A. Starykh, A. V. Chubukov, and A. G. Abanov, Phys. Rev. B **74**, 180403(R) (2006).
[33] W. H. Zheng, J. O. Fjærestad, R. R. P. Singh, R. H. McKenzie, and R. Coldea, Phys. Rev. B **74**, 224420 (2006).
[34] A. L. Chernyshev and M. E. Zhitomirsky, Phys. Rev. B **79**, 144416 (2009).